WATER RESOURCES RESEARCH, VOL. 25, NO. 1, PAGES 126–134, JANUARY 1989

Regional Scale Transport in a Karst Aquifer 2. Linear Systems and Time Moment Analysis

SHIRLEY J. DREISS

Department of Earth Sciences, University of California, Santa Cruz

Travel time distributions of water or tracers in conduit-type karst aquifers can be found from linear systems analysis of either tracer test data or naturally occurring fluctuations in springflow chemistry. I use the chemical fluctuations at Maramec Spring, Missouri described in paper 1 (Dreiss, this issue) and results from a previous tracer test to derive a set of kernal functions that represent regional scale transport in the karst conduit network. A single kernel is sufficient to simulate the storm-derived component of Maramec springflow, suggesting that rapid transport in the conduit network is well-approximated by temporal stationarity. Time moment analysis of the kernels leads to several conclusions. The kernel for the tracer test exhibits a larger mean residence time and much smaller variance than the kernels derived from nonpoint source recharge. Thus the tracer travel distance appears to be longer than the mean travel distance of rapid recharge and much of the variance of nonpoint source kernels apparently results from the distribution of flow path lengths to the spring. By assuming an effective transport model and comparing the moments of the empirical tracer test kernel to the moments of the impulse response of the model, I compute an effective velocity between the tracer input point and Maramec Spring of 1.3 km/day and an effective dispersivity of 0.29 km. Because the time moments of the kernels and the effective transport parameters can be computed from readily measured springflow properties, they may prove to be a convenient means for studying and comparing regional scale transport in karst aquifers.

INTRODUCTION

In many karst aquifers, sparsely distributed solution features control rates and directions of a large portion of the regional groundwater flow. Water quickly infiltrates after storm events and some of the infiltration moves rapidly through a network of solution conduits to spring outlets. In the first paper [*Dreiss*, this issue], I estimated amounts of recent, storm-derived water in the discharge of a spring in southeastern Missouri. Using measured chemical perturbations in the spring flow, I found that rapidly transmitted water comprised approximately 25% of the total spring discharge. Relatively dilute water began to arrive at the spring within 1 day after each large storm event. The dilute component reached a maximum during the recession of the springflow hydrograph, about 2–5 days after the events.

This type of discrete conduit flow cannot be described with continuum models for flow through porous media because the representative elementary volume for the conduit network is undefined and likely to be very large. Similarly, models of flow in individual conduits are not feasible because the location and geometry of the conduits are unknown. Here, I present an application of linear systems and time moment analysis to the spring discharge and cation concentration measurements from southeastern Missouri. The systems approach is well-suited to studies of karst aquifers because it describes regional scale transport in terms of the distribution of travel or residence times without requiring detailed knowledge of the internal structure of the aquifer.

In this paper, I treat the observed chemical fluctuations at Maramec Spring as naturally occurring, regional tracer events that represent the response of the karst aquifer to a series of nonpoint source inputs. Examples of kernel function identification are presented using five sets of data: a long-term, 12-month sequence, three short-term subsets of the record, and a tracer test previously performed at the spring. I then compare time moments of the kernels and discuss them in the context of two alternative approaches for describing karst aquifers: (1) the conceptual classification sheme of diffuse and conduit-type aquifers and (2) a dual-porosity, convective-dispersive transport model.

Paper number 88WR03221.
0043-1397/89/88WR-03321$05.00

BACKGROUND

Linear systems analysis has been used for many years in hydrology to describe rainfall-runoff relationships and in chemical engineering to interpret reactor performance [e.g., *Dooge*, 1973; *Himmelblau and Bischoff*, 1968]. Recently, several studies have proposed the use of linear transfer functions to describe regional scale solute transport in fractured aquifers and highly heterogeneous soils [*Duffy and Harrison*, 1987; *Jury et al.*, 1986; *Rinaldo and Gambolati*, 1987]. The problems encountered in modeling these processes are similar to those in karst hydrology.

Linear systems analysis was first applied to karst aquifers by *Knisel* [1972] and *Dreiss* [1982, 1983] in studies that considered excess precipitation as an input time series and spring discharge as an output series. The identified kernel functions in these studies were analogous to instantaneous unit hydrographs for surface runoff.

Recently, *Duffy and Gelhar* [1986] applied spectral analysis to tritium concentration histories to identify a kernel function and phase spectra for transport to a spring in a karst region of the Swiss Alps. They then compared the frequency distribution of the empirical transfer function to that of a one-dimensional, convective-dispersive model to obtain estimates of the primary karst reservoir volume and the dispersivity of the system. The investigation used biweekly tritium measurements in a region with significant snowmelt contributions. The accuracy of the study results may have been effected by the long sampling interval [see *Dreiss*, this issue] and the difficulty of estimating the input series because of snowpack storage of

tritium. Nevertheless, the approach is similar to the one presented here. The major differences are that *Duffy and Gelhar* [1986] use frequency domain analysis of biweekly isotope data and an effective dispersion model, and this study utilizes discrete deconvolution of daily cation concentrations and time moment analysis of the resulting kernel.

LINEAR SYSTEMS ANALYSIS

If assumptions of linearity and time invariance are made, the observed fluctuations in the chemical composition of spring flow can be analyzed by treating the karst conduit system as a linear filter which transforms a series of input stimuli into output responses (Figure 1). In this case, the input values are rapid infiltration rates into the conduit network. Outputs are flowrates of storm-derived, relatively dilute water arriving at the spring outlet.

For a linear, time-invariant system, a single empirical transfer function or kernel function, which reproduces the observed behavior of the physical system, can be identified from known or measured input and output time series. In tracer tests, where the input and output series are the mass rate of solute entering and leaving the system, respectively, the kernel function represents both the residence time distribution of the solute in the system, and the probability distribution of solute travel times.

Kernel Function Identification

The behavior of a linear, time-invariant system is described by the convolution integral

$$y(t) = \int_0^t h(t - \hat{t})x(\hat{t})\, d\hat{t} \tag{1}$$

where $y(t)$ is the continuous system response, $x(\hat{t})$ is the input series, and $h(t - \hat{t})$ is the kernel function [*Dooge*, 1973]. For discrete, noisy measurements, (1) becomes

$$y_i = \Delta t \sum_{j=0}^{i} x_j h_{i-j} + e_i \qquad i = 0, 1, 2, \cdots, N \tag{2}$$

for $N + 1$ output data points collected at intervals of equal length Δt. Output values at times $i\Delta t$ are y_i. The x_j and h_i represent mean input and kernel function values over time step intervals Δt. The error terms e_i are residuals due to measurement errors, or, if model assumptions are not strictly met, nonlinearities and temporal changes in the system.

The sensitivity of kernel function identification to inaccurate data and nonlinearities has been demonstrated by a number of researchers [e.g., *Blank et al.*, 1971; *Delleur and Rao*, 1971; *Laurenson and O'Donnell*, 1969]. If there is error in the data, the identification problem becomes one of finding an optimum kernel function using all available information. Methods of least squares, time series analyses and mathematical programming are most commonly applied to this problem [e.g., *Eagleson et al.*, 1966; *Neuman and de Marsily*, 1976; *Kanasewich*, 1975].

In this study, we find h_{i-j} by minimizing the sum of the square of the errors E

$$\min E = \sum_{i=0}^{N} e_i^2 \tag{3}$$

subject to the constraints that the discrete kernel is nonnegative:

$$h_k \geq 0 \qquad k = 0, 1, 2, \cdots, M \tag{4}$$

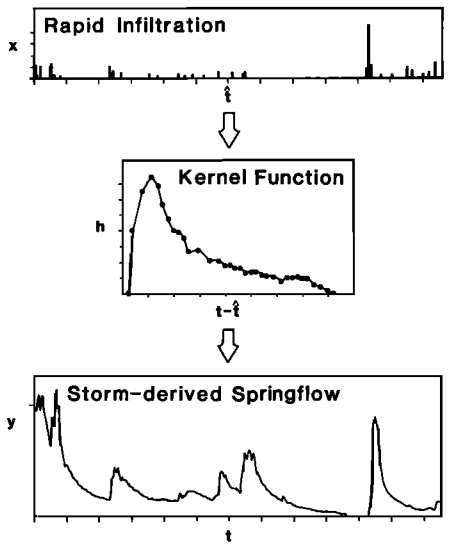

Fig. 1. Schematic diagram of linear systems analysis of karst conduit-type spring flow.

where M is the memory length of the system. Equations (2) through (4) are solved using a constrained least squares procedure similar to that described by *Kanasewich* [1975].

When the total volumes of the input and output series are equal, the area under the kernel is unity

$$\Delta t \sum_{k=0}^{M} h_k = 1 \tag{5}$$

and the h_k represent the response of the system to an instantaneous unit input. In applications to karst aquifers, the shape of the kernel function represents the age distribution of water in the conduit network and the distribution of solute travel times for regional scale transport through the network. For example, the fraction of spring flow of age equal to or less than t' is the integral of the kernel between 0 and t', or approximately,

$$\Delta t \sum_{k=0}^{t'} h_k \tag{6}$$

and the fraction older than t' is approximately

$$\Delta t \sum_{k=t'+\Delta t}^{M} h_k \tag{7}$$

Time moments of the kernel describe the shape of the function and the statistical properties of the travel or residence time distribution.

Time Moment Analysis

The method of moments is widely used in time series analyses [e.g., *Priestly*, 1981] and has recently been applied in studies of transport through porous media [e.g., *Valocchi*, 1985; *Goltz*, 1986]. The basic premise of time moment analysis is that the shape of a downstream response of a system observed at point x may be described by a set of moments

$$\mu_n(x) = \int_0^\infty t^n \eta(x, t)\, dt \tag{8}$$

where $\mu_n(x)$ is the nth moment about the origin at location x, t is time, and $\eta(x, t)$ is the observed disturbance [*Aris*, 1958]. In

the context of the kernel for a karst aquifer, the h_k describe the response of the conduit system to an instantaneous unit input located a distance x from the spring. The zeroth order moment μ_0 is the area under the kernel, which in this case is equal to 1.

The first moment of h_k, approximated for discrete data as

$$\mu_1 = \Delta t \sum_{k=0}^{M} k h_k \tag{9}$$

is the centroid of the area under the kernel. The quantity μ_1/μ_0 has dimensions of time and is the mean residence time $\bar{t}$ of water traveling to the spring.

The amount of spreading or mixing in the system response is described by the variance σ^2 of the response, which is the second central moment about $\bar{t}$

$$\sigma^2 = \Delta t \sum_{k=0}^{M} (k - \bar{t})^2 h_k \tag{10}$$

or nondimensionality as the coefficient of variation C_v, where

$$C_v = \sigma/\bar{t} \tag{11}$$

Values of σ^2 and C_v are related to the distribution and interconnectedness of travel pathways in a system. Kernel functions for an aquifer with a narrow distribution of pathways will exhibit less variance than those for an aquifer with a broad pathway distribution. Similarly, the variance of h_k will be larger for aquifers where travel pathways are highly interconnected and smaller for aquifers, such as conduit-type karst aquifers, where large quantities of water are transmitted rapidly in discrete conduits. Thus the variance should be larger for springs in less mature karstic terranes and in aquifers with large recharge areas.

The skewness of h_k can be expressed as the third central moment Γ where

$$\Gamma = \Delta t \sum_{k=0}^{M} (k - \bar{t})^3 h_k \tag{12}$$

or, nondimensionality, as the skewness coefficient γ,

$$\gamma = \Gamma/\sigma^3 \tag{13}$$

Skewness results from at least three phenomena: (1) increasing dispersion with time as the response passes the observation point, (2) a nonsymmetric distribution of travel distances, and (3) delay effects from storage in relatively immobile portions of the aquifer. The first of these becomes less important with increasing fluid flow velocities. The second depends on the distribution of distances between points of rapid recharge and the spring outlet. The third develops as water enters and leaves dead-end solution conduits, fine pores, and fractures in response to changes in fluid pressures in the conduits.

APPLICATIONS

Daily precipitation, spring discharge, and cation concentration measurements were made at Maramec Spring during a 375-day period between November 1985 and November 1986. Here I use those data, as well as the results from a tracer test at the spring, to identify kernel functions for transport through the karst aquifer.

1985–1986 Record

First, consider the full-length data record shown in Figure 2 in the first paper [*Dreiss*, this issue], in which I used spring flow and cation concentration measurements to estimate Q_{new}, the mean daily flowrate of storm-derived water arriving at the spring outlet [*Dreiss*, this issue, Figure 6]. That series is used here as the output response y_i in the kernel identification (Figure 2).

The input sequence x_j is an excess precipitation series, scaled so that the total volume of the input and output series are equal. Excess precipitation in this case refers to the total measured precipitation less evapotranspiration losses computed with a Thornthwaite moisture balance [*Thornthwaite and Mather*, 1957]. In karst regions, this excess precipitation contributes both to surface runoff and to groundwater circulation in the conduit network. A portion of the groundwater circulation feeds to spring outlets and the remainder leaves as deep groundwater circulation out of the region. To avoid the difficulty of estimating separate surface runoff, spring flow, and deep circulation components, a constant fraction of each excess daily precipitation event is assumed to eventually reach the spring outlet. The x_j are computed by scaling the daily excess precipitation series by a factor equal to the ratio of the total output volume to the total volume of excess precipitation. Thus the total volume of the scaled input series is equal to the volume of the output response and the computed kernel function represents a unit response function of the conduit network.

Initially, I identified an optimal kernel function from x_j and y_i using (2) through (4) with a nonnegativity constraint but no memory length specification. Figure 2 shows the computed kernel and its ability to reproduce y_i. The kernel was not smoothed and has an apparent memory length of 223 days and a maximum at $k = 5$ days. It simulates the output series well, with an average absolute error of 0.56 m^3/s, where the average error is defined as the sum of the absolute differences between y_i and the simulated output values divided by N. The beginning of the sequence is underestimated by the kernel because the observed y_i include discharge from storms that occurred prior to the start of the record.

The kernel exhibits large initial values between 0 and 40 days and a tail of smaller values between 40 and 223 days. The first moment of h_k, the mean residence time, is 69.1 days. The second and third moments C_v and γ are 0.72 and 0.75, respectively.

The h_k for $k > 40$ days could reflect relatively long travel times for transport through the karst network. However, this tail portion of the kernel is approximately 6 months long and could also result from seasonal errors in the estimation of x_j or y_i. For example, in computing y_i, prestorm Ca ion concentrations C_{old} were assumed to be constant throughout the monitoring period at the maximum measured Ca concentration of 36.9 mg/L [*Dreiss*, this issue]. C_{old} might actually change seasonally, becoming lower during times of high infiltration and higher after long periods with no infiltration. If this is the case, but only the late summer maximum C_{old} has been used to compute y_i, the output series will be overestimated during periods of high infiltration.

To demonstrate the effect of a seasonally varying C_{old} on the computed y_i and h_k, a new series y_i^* was formed using C_{old} values that fluctuate on an annual cycle (Figure 3). C_{old} was assumed to vary between the maximum measured calcium concentration, 36.9 mg/L on September 29 and 30.3 mg/L measured 182 days previously on March 31. This value was measured exactly half a year before the maximum concentration and was close to the minimum measured value in

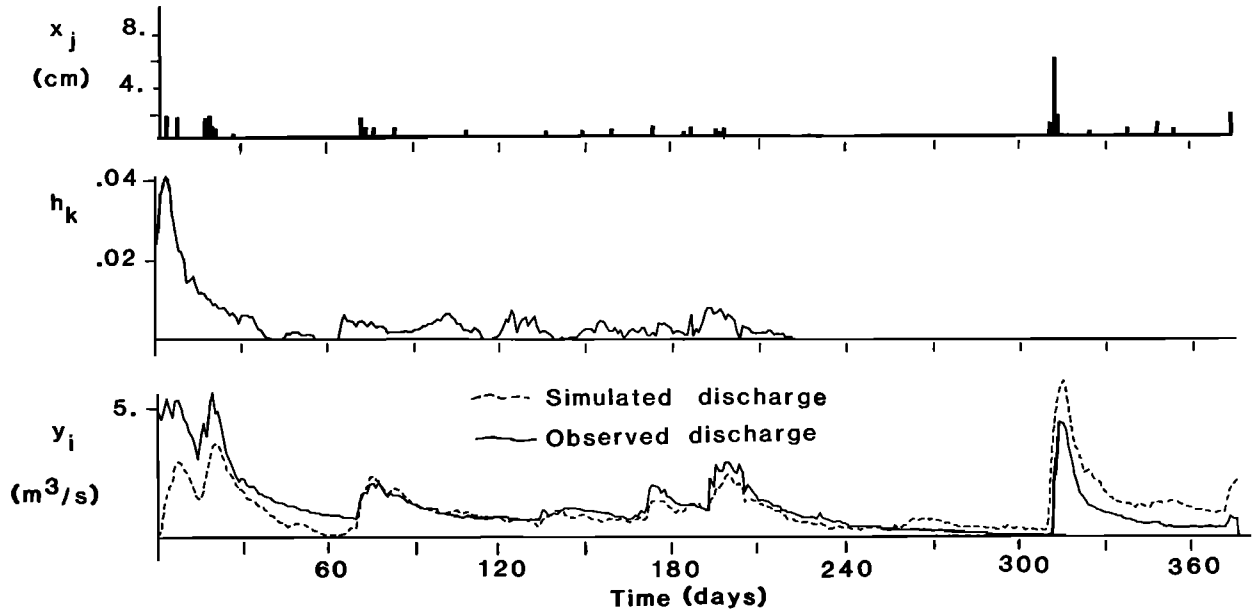

Fig. 2. Input series x_t, output series y_t, and kernel function h_k derived with no memory constraint from the full-length record at Maramec Spring.

the series. The corrected C_{old}* is a cosine function with a wavelength of 364 days and an amplitude of 3.3 mg/L:

$$C_{old}^*(i) = \bar{C} + (36.9 + \bar{C}) \cos\left[\frac{(n\text{day} - 309)2\pi}{364}\right] \quad (14)$$

$$i = 1, 2, \cdots, N$$

where $\bar{C}$ is (36.9 + 30.2)/2, $n$day is the number of days since the start of the record, and 309 is the number of days to the date of maximum concentration.

Figure 3 illustrates the new y_t* and kernel functions identified from y_t* and the original x_j series. Again, the kernels were identified from (2) through (4). No memory length was specified in deriving the h_k in Figure 3*a*. The seasonal correction in

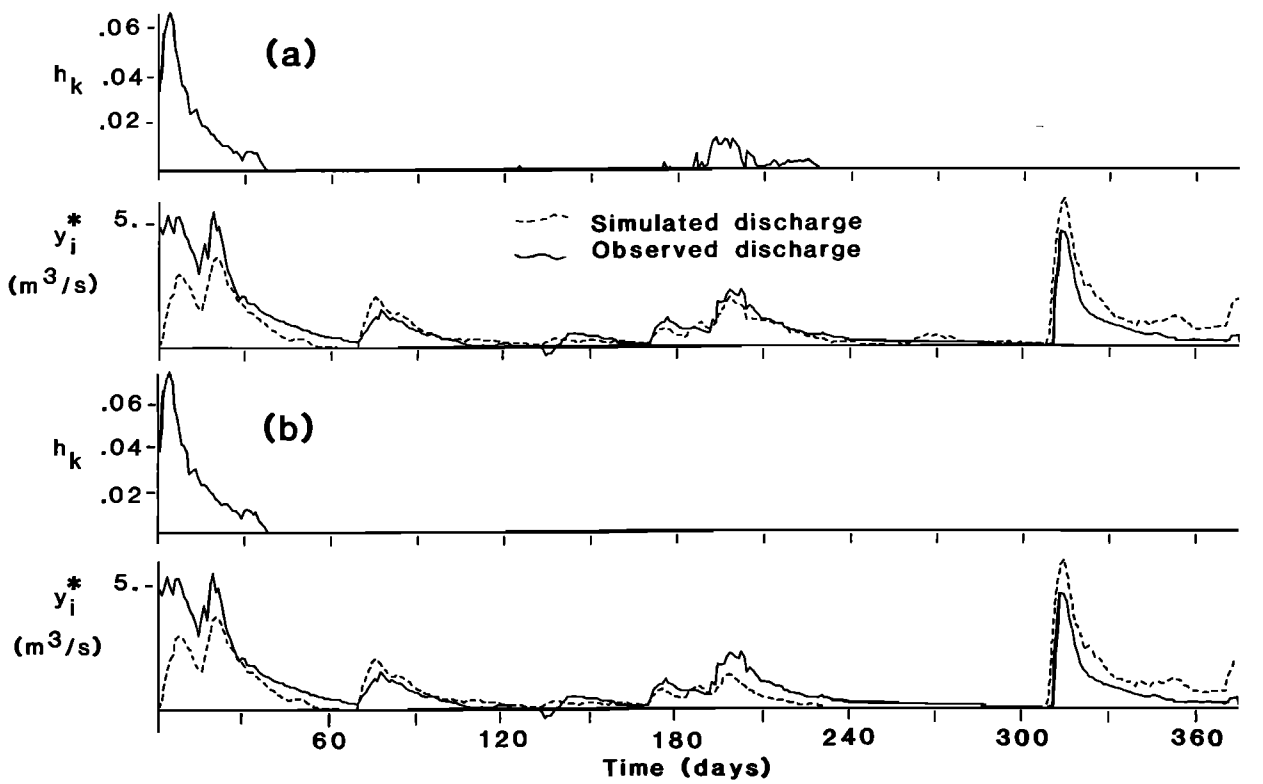

Fig. 3. Kernel functions derived from full-length record at Maramec Spring using C_{old}* correction with (*a*) no memory constraint and (*b*) M = 40 days.

the output series eliminates the tail in the derived kernel function except for a series of values between 175 and 230 days. These values are associated with a disproportionately large spring flow response after several relatively small precipitation events. Specifying the memory of the h_k to be 175 days or less truncates these values but does not alter the shape of the main part of the kernel (Figure 3*b*). In this case, the kernel has a memory of only 38 days and reproduces the output response well with the exception of the response between 175 and 230 days. The h_k derived with the memory constraint exhibit a maximum at $k = 5$ days, with an average absolute error of 0.50 m^3/s. The shorter memory length is reflected in the computed time moments. The $\bar{t}$ for the new kernel is 11.8 days. The C_v is 0.77 and γ is 1.01.

Although seasonal variations in C_{old} are a plausible cause of the extended tail of the kernel, other types of seasonal effects could also account for the tail. For example, the calculated excess precipitation in the Thornthwaite moisture balance uses an empirical relationship between day length, temperature, and evapotranspiration. If this relationship is inaccurate for southeastern Missouri, x_j will contain seasonally varying errors that could cause the tail of the kernel. However, if this were the case, it is likely that the frequency as well as the magnitude of the input events would be poorly estimated by the Thornthwaite moisture balance. Input events would occur in the x_j series when no corresponding output responses were present in the y_i. Also, the timing and number of peaks in the simulated output series, computed by convolving h_k and x_j, would differ from those in the observed y_i series. Because this does not occur in the Maramec data, errors in the moisture balance are probably not the cause of the kernel function tail, and variations in C_{old} are the most plausible cause of the seasonal effects.

Short-Term Storm Sequences

The kernels in Figures 2 and 3 generally reproduce y_i or y_i^* well. This suggests that the residence time distribution of water in the conduit system changes little with the time of year or with the magnitude and pattern of precipitation events. If this is true, the shape and moments of h_k derived for individual storms of different magnitude or for periods with relatively high or relatively low infiltration should be similar.

To investigate the temporal stationary of h_k, we identified kernels for three subsets of the data record. The sequences are each preceeded by 40 days or more with little or no excess precipitation and extend more than 40 days after the last major input event. In each example, the storm-derived spring flow was computed with the C_{old}^* in (14) and is a portion of the y_i^* series in Figure 3.

Figure 4 compares the derived kernels for the short-term sequences and the kernel for the long-term sequence in Figure 3*b*. The average absolute error in reproduction of y_i^* ranges between 0.15 m^3/s for the most complex series in April/June and 0.01 m^3/s for the October/November series (Table 1). The kernels are visually similar, with peaks occurring between 5 and 8 days after a storm event and memory lengths in the range of 33 to 41 days.

The kernel for the April/June storm sequence exhibits a longer $\bar{t}$ and a less distinct peak than the other kernels. This data subset includes the June response that was poorly simulated by the kernel for the long-term record. The estimated excess precipitation events just prior to the June storm response are small in comparison to the associated discharge response and, apparently, are poor estimates of the actual infiltration that created that response. To compensate for the apparent input errors, the tail of the derived kernel has relatively high values. Thus the kernel for the April/June subset is probably a less accurate representation of transport in the aquifer than the kernels for the long-term or other short-term sequences.

The similarity between the moments of the kernels for the February/March, the October, and the corrected full-length records is striking (Table 1); the $\bar{t}$ range between 11.1 and 11.8 days, C_v between 0.68 and 0.77, and γ between 0.83 and 1.14. This consistency suggests that a single linear kernel adequately describes transport through the system when the inputs are nonpoint source precipitation events.

Tracer Test

The kernels in Figure 4 represent arrival times for basin scale transport from nonpoint sources. They depict travel along numerous pathways, over a distribution of travel distances, as well as transport processes such as dispersion along individual pathways. To illustrate and compare a kernel from a point source to the nonpoint source kernels, we examined the results of a tracer test conducted in an earlier study at Maramec Spring.

In May 1982, *Vandike* [1984] placed Rhodamine dye in a creek bed approximately 21 km from the spring. Dye began arriving at the spring 11 and 12 days later and continued to be present in the spring water for at least 12 days. The input for the kernel identification is an instantaneous unit input at the time of the tracer injection. The output responses y_m are the mass rate of arrival of the dye, normalized by the total mass that arrived at the spring outlet,

$$y_m = \frac{q_m C_m \Delta t}{\sum_{m=1}^{N} q_m C_m \Delta t} \qquad m = 1, 2, \cdots, N \tag{15}$$

where N is the total number of sampling intervals and m is the number of intervals since the start of the test. The q_m are the mean daily springflows during the mth intervals and C_m are the measured dye concentrations. In this case, y_m is a unit response to the tracer injection and

$$h_k = y_m \qquad k = m = 1, 2, \cdots, M \tag{16}$$

The derived kernel and its moments are included in Figure 4 and Table 1. The mean residence time of the tracer is 16.0 days. This is 4–5 days greater than the $\bar{t}$ of the nonpoint kernels and indicates that the travel distance of the tracer was longer than the mean travel distance of rapid infiltration. C_v of the tracer kernel is 0.19, much smaller than the nonpoint source kernels, suggesting that much of the variance in the nonpoint source kernels is due to the distribution of flowpath lengths to the spring. On the other hand, the γ of the tracer kernel is 0.96, similar to values for the nonpoint kernels. Thus the skewness appears not to be sensitive to the travelpath distribution or the path length distribution.

DISCUSSION

Physical interpretations of the moments can be discussed further in the context of two alternative models for transport in karst aquifers. One approach is based on the qualitative description of karst aquifers as either diffuse or conduit types

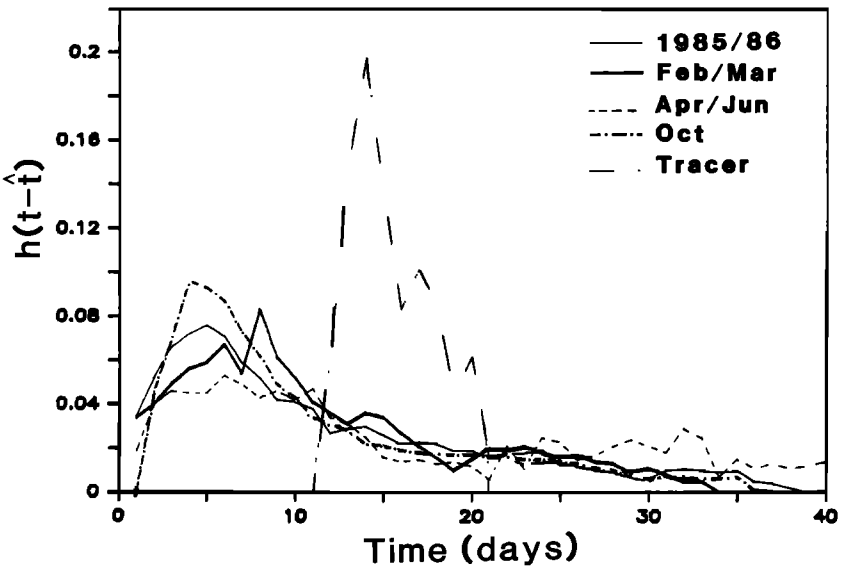

Fig. 4. Comparison of kernel functions derived from the long-term record, short-term data subsets, and tracer test results.

and an analogy between this classification scheme and a mixing cell model. The mixing cell model is not physically realistic but provides a straightforward, alternative means of describing the degree of mixing in the aquifer. A second approach is a deterministic model for transport in dual-porosity porous media similar to those used to describe solute transport in unsaturated soils. The model is more physically detailed and allows effective transport properties, i.e., effective dispersivity and velocity, to be defined and to be estimated from the time moments of the kernel functions.

Diffuse and Conduit Aquifer Classification

Shuster and White [1971] proposed a method for qualitatively classifying karst aquifers as either "diffuse" or "conduit" type aquifers depending on several properties of the aquifers and springs. In diffuse flow aquifers, springs are usually small and controlled by stratigraphic and structural features. Spring chemistry does not vary seasonally or after storm events. In conduit aquifers, the specific conductivity of springflow is highly variable, seasonally and after large storm events. Groundwater flow occurs in solution conduits and is sometimes described as "pipe flow" or "plug flow."

This very useful conceptual method for describing karst aquifers can be interpreted in terms of the degree of mixing that occurs within the aquifer. Purely conduit-type aquifers or purely diffuse aquifers are end members of the spectrum of aquifers that actually occur in nature. In a purely diffuse flow aquifer, recharge is completely mixed with preexisting water in the aquifer, so the spring flow shows very little variation in chemistry over time. In contrast, pure conduit flow results in little mixing and therefore large temporal variation in spring flow chemistry.

Diffuse and conduit aquifers might be conceptualized as end-members of a set of mixing cell models where the degree of mixing is represented by a series of mixing cells as shown in Figure 5*a*. The material balance in each cell is [*Himmelblau and Bischoff*, 1968]

$$V' \frac{dc_i}{dt} + Qc_i = Qc_{i-1} \qquad i = 1, 2, \cdots, l \tag{17}$$

where $c_i(t)$ is the tracer concentration in the ith cell, V' is the volume of an individual cell, Q is a constant flow rate, and l is the number of cells in the model. A kernel function for a

TABLE 1. Time Moments for Storm Sequences and Tracer Test

Date	N, days	C_{old}, mg/L	M, days	Average Absolute Error, m^3/s	$\bar{t}$, days	C_v	γ
November 1985 to November 1986	375	36.9	223	0.56	69.1	0.72	0.75
November 1985 to November 1986	375	(14)	38	0.50	11.8	0.77	1.01
February–March 1986	61	(14)	33	0.06	11.7	0.68	0.83
April–June 1986	175	(14)	41	0.11	16.2	0.71	0.55
October 1986	38	(14)	36	0.01	11.1	0.74	1.14
Tracer	25	NA	14	0.00	16.0	0.19	0.96

NA, not applicable.

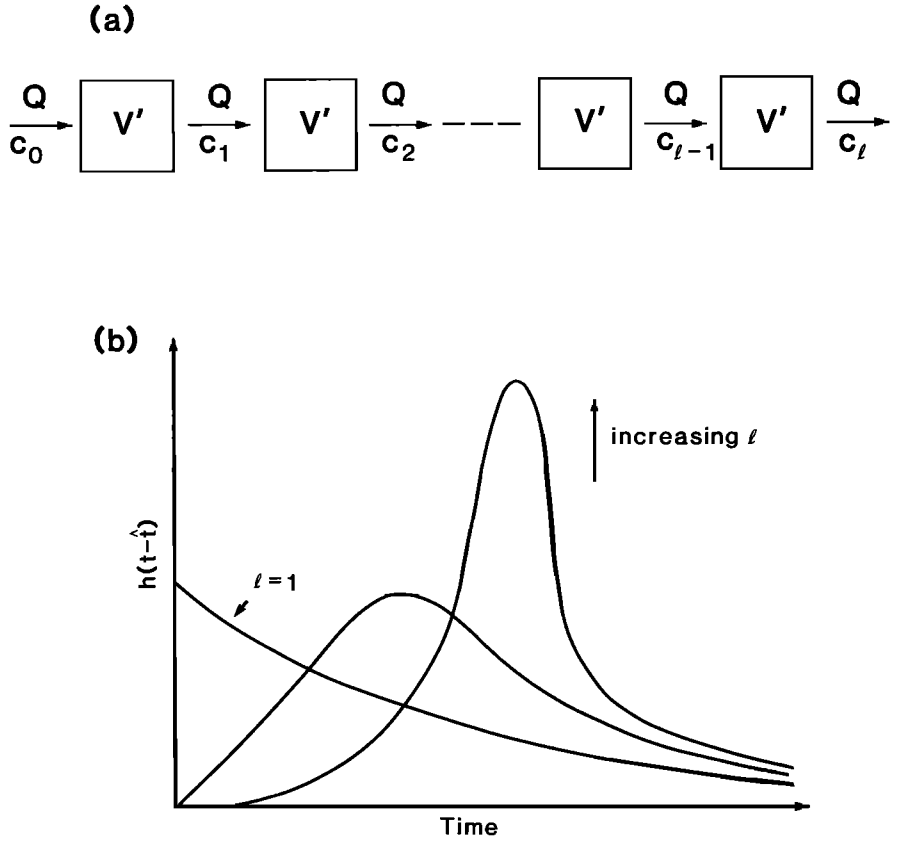

Fig. 5. Illustration of (*a*) the mixing cell model and (*b*) the change in kernel function shape with increasing number of cells (adapted from *Himmelblau and Bischoff* [1968]).

model with l mixing cells is found by solving (17) for an instantaneous input into cell 1 under initial conditions of no tracer present

$$c_{i\neq 0}(0) = 0 \qquad c_{i=0}(t) = c^*(t)[V/Q]\delta(t) \tag{18}$$

where $c^*(t)$ is the average concentration of tracer if distributed throughout system. V is the total volume of all cells and is equal to lV', and $\delta(t)$ represents a dirac delta function.

Figure 5*b* schematically illustrates shapes of kernel functions for systems with different degrees of mixing modeled by a series of mixing cells. As the number of cells in the model increases, the degree of mixing decreases. Time moments of kernels of the mixing cell model also depend on the number of mixing cells [*Himmelblau and Bischoff*, 1968]

$$\mu_n = \frac{(n+l-1)(n+l-2)\cdots(l)}{(l)^n} \tag{19}$$

and C_v is

$$C_v = (1/l)^{1/2} \tag{20}$$

For the ideally mixed case, l is 1, and C_v is 1. For plug flow, $l \to \infty$ and $C_v \to 0$.

Kernel functions and time moments for real aquifers fall within these two extremes. Kernel functions for conduit flow aquifers should have relatively low variance and fit models with a large number of mixing cells. For example, the C_v of the kernel for the tracer test at Maramec Spring is 0.19 and therefore from equation (19), the tracer test results will fit a mixing cell model with approximately 27 cells.

Although the mixing cell model oversimplifies transport in karst aquifers, it illustrates the relationship of the derived kernel functions and time moments to the diffuse and conduit flow classification scheme. Clearly, the variance of the kernels represents the degree of mixing that occurs within the aquifer. The higher the variance of the kernel, the lower the number of mixing cells required to fit the aquifer response, and the greater the degree of mixing in the aquifer. Similarly, the lower the variance, the closer the aquifer approaches the conduit-type end-member in the classification scheme.

Dual-Porosity Transport Model

A more physically detailed model might consider the karst aquifer as dual-porosity media composed of regions of relatively mobile and immobile storage. The mobile storage is the conduit network and immobile storage includes fine fractures, pores, and dead-end cavities. Water and associated solutes travel rapidly in karst conduits, but some transfer occurs between the conduits and adjacent fractures and pores. This process may have a similar effect on solute transport through the conduit network as observed in soils with immobile phases. At short distances, tracer tests in soil columns exhibit early arrival times and subsequent tailing in the breakthrough curves. At greater distances, the breakthrough curves have more regular shapes and larger associated dispersion coefficients.

The time moments of the tracer test kernel can be used to compute regional scale, effective transport parameters by, first, assuming a model for convective-dispersive transport, then

comparing the empirical moments to the moments of the impulse response of the model. *De Smedt and Wierenga* [1984] describe one-dimensional transport in dual-porosity media in the context of flow in unsaturated soils. As an example, we apply their approach here to interpret the kernel function from the Maramec Spring tracer test.

For one-dimensional flow through porous media with mobile and immobile regions, *De Smedt and Wierenga* [1984] describe transport in the mobile fraction by the expression

$$\phi \frac{\partial C_m}{\partial T} = \frac{1}{P_m} \frac{\partial^2 C_m}{\partial X^2} - \frac{\partial C_m}{\partial X} - \frac{C_m - C_{im}}{P_{im}} \tag{21}$$

and a simple mass transfer relationship for transfer into and out of stagnant zones

$$(1 - \phi) \frac{\partial C_{im}}{\partial T} = \frac{C_m - C_{im}}{P_{im}} \tag{22}$$

where $X = z/L$, $T = vt/L$, $P_m = v_m L/D_m$, $P_{im} = v_m/L\alpha$, and $\phi = \theta_m/\theta$; θ_m and θ_{im} are volumetric fractions of mobile and immobile water content, and C_m and C_{im} are solute concentrations in mobile and immobile water. D_m is the hydrodynamic dispersion coefficient in the mobile phase, v_m is the average mobile flow velocity, α is a mass transfer coefficient, and L is the length of the porous media. The distance along the flow path is z and v is average seepage velocity.

Passioura [1971] demonstrated that for flow in cylindrical pore spaces whose length is much larger than their radius, the mass transfer equation is not necessary if the mobile phase dispersion coefficient is redefined to include effects of both mobile and immobile transfer. Solute transport in the mobile phase can then be approximated by

$$\frac{\partial C_m}{\partial T} = \left[\frac{1}{P_{\text{eff}}}\right] \frac{\partial^2 C_m}{\partial X^2} - \frac{\partial C_m}{\partial X} \tag{23}$$

where

$$\frac{1}{P_{\text{eff}}} = \frac{1}{P_m} + (1 - \phi)^2 P_{im} \tag{24}$$

From the definition of the Peclet numbers, the effective dispersion coefficient D_{eff} is

$$D_{\text{eff}} = \phi D_m + \frac{(1 - \phi)^2 v_{\text{eff}}^2}{\phi \alpha} \tag{25}$$

where v_{eff} is the average effective flow velocity, $v_{\text{eff}} = v_m \phi$. *De Smedt et al.* [1981], *Baker* [1977], *Rao et al.* [1980], and others have applied this approach to transport through soils and aggregated porous media with variable pore sizes.

Effective transport properties for the karst aquifer can be computed by comparing the first and second moments of the tracer test kernel function to the moments of the unit impulse response of the dual-porosity model. Following the approach of *Aris* [1958] and *Valocchi* [1985], the first and second moments of (23) are found to be

$$\bar{t} = \bar{x}/v_{\text{eff}} \tag{26}$$

$$\sigma^2 = 2D_{\text{eff}}\bar{t}/v_{\text{eff}} \tag{27}$$

where $\bar{x}$ is the average linear travel distance of a solute or tracer.

The D_{eff} and v_{eff} for a given travel distance can be computed directly from the empirical values of t and C_v. For example, for an approximate travel distance of 21 km between the tracer input location and Maramec Spring, $v_{\text{eff}} = 1.3$ km/day and $D_{\text{eff}} = 0.38$ km^2/day. The effective dispersivity, defined as

$$\alpha_{\text{eff}} = D_{\text{eff}}/v_{\text{eff}} \tag{28}$$

is 0.29 km. This value is about two orders of magnitude smaller than the dimensions of the spring recharge basin, which is approximately 20 km wide and 50 km long. D_{eff} and v_{eff} are regional scale, temporal, and spatial averages that do not represent the discrete features in the karst aquifer. Thus a convective-dispersive model using these regional scale properties should be applied with caution when simulating transport in the karst conduit system at short times or close to the source of contamination. Nevertheless, the effective parameters provide an additional means for comparing transport processes between different locations within a single karst aquifer or among different karst aquifers.

Summary and Conclusions

A number of observations and conclusions can be made from analysis of the derived kernel functions and a comparison of the functions to alternative models for transport in karst aquifers.

1. A single linear kernel function is sufficient to simulate the storm-derived component of Maramec springflow for both long- and short-term storm sequences. Thus rapid transport to the spring of nonpoint source precipitation is well-approximated as stationary in time.

2. Ca concentrations in the secondary porosity component of Maramec spring flow appear to vary seasonally. This variation may be the result of seasonal mixing of rapidly recharged, relatively dilute water with preexisting water in less mobile storage in fractures, pores, and dead-end cavities.

3. The kernels derived from the spring flow storm responses represent the residence time distribution of rapid groundwater recharge in the conduit network. Because the recharge source is areally distributed, the kernels describe regional scale transport over numerous pathways and a distribution of travel distances. The kernel function derived for a tracer test at Maramec Spring has a larger mean residence time and much smaller variance than the storm response kernels. This implies that the travel distance of the tracer was longer than the mean travel distances of rapid infiltration and that much of the variance in the nonpoint source kernels results from the distribution of flow path lengths to the spring. The skewness values for the kernels are similar, suggesting that the skewness is not sensitive to the distribution of travel path lengths.

4. The time moments of the kernels are a convenient means of describing mean travel times and the degree of mixing that occurs during rapid transport in the aquifer. Kernels for conduit-type aquifers, such as the one studied here, should have a relatively low variance, reflecting the fact that little mixing takes place during transport.

5. Regional scale, effective transport properties can be computed directly from the moments of a tracer test kernel by assuming an effective transport model and comparing the moments of the empirical kernel to the moments of the impulse response of the model. Following this procedure for the Maramec tracer test, we computed an effective velocity between the tracer input point and Maramec Spring of 1.3 km/day and an effective dispersivity of 0.29 km.

6. The principal advantage of the time moment approach is that it describes regional scale transport through a karst aquifer under natural conditions using readily measured spring flow properties. This approach should prove to be an informative method for studying and comparing transport in karst aquifers.

Acknowledgments. Numerous discussions with colleagues helped to crystallize the ideas presented here. The author is particularly indebted to James Vandike of the Missouri Department of Natural Resources for providing detailed information on the Maramec Spring tracer test, and to Steven Ward, who wrote the programs to perform the kernel identifications. Computations were performed on the Richter Seismology Laboratory VAX 11-750 at The University of California, Santa Cruz. The project was supported by a grant from the Environmental Geosciences Program of the National Science Foundation, grant EAR 8307686-01.

REFERENCES

Aris, R., On the dispersion of linear kinematic waves, *Proc. R. Soc. London, Ser. A, 245*, 268–277, 1958.

Baker, L. E., Effects of dispersion and dead-end pore volume in miscible flooding, *Soc. Pet. Eng. J., 17*, 219–227, 1977.

Blank, D. J., J. W. Delleur, and A. Giorgini, Oscillatory kernel functions in linear hydrologic models, *Water Resour. Res., 7*(5), 1101–1117, 1971.

Delleur, J. W., and R. A. Rao, Linear systems analysis in hydrology—The transform approach, the kernel oscillations and the effect of noise, in *Systems Approach in Hydrology*, pp. 116–142, Water Resources Publishers, Fort Collins, Colo., 1971.

De Smedt, F., and P. J. Wierenga, Solute transfer through columns of glass beads, *Water Resour. Res., 20*(2), 225–232, 1984.

De Smedt, F., P. J. Wierenga, and A. Van der Beken, Theoretical and experimental study of solute movement through porous media with mobile and immobile water, *Rep. VUB-Hydrol., 6*, 219 pp., Univ. Brussels, Belgium, 1981.

Dreiss, S. J., Linear kernels for karst aquifers, *Water Resour. Res., 18*(4), 865–876, 1982.

Dreiss, S. J., Linear unit-response functions as indicators of recharge areas for large karst springs, *J. Hydrol., 61*, 31–44, 1983.

Dreiss, S. J., Regional scale transport in a karst aquifer, 1, Component separation of spring flow hydrographs, *Water Resour. Res.*, this issue.

Dooge, J. C. I., Linear theory of hydrologic systems, U.S. Dep. of Agric., *Tech. Bull. 1468*, Washington, D.C., 1973.

Duffy, C. J., and L. W. Gelhar, A frequency domain analysis of groundwater quality fluctuations: Interpretation of field data, *Water Resour. Res., 22*(7), 1115–1128, 1986.

Duffy, C. J., and J. Harrison, The statistical structure and filter characteristics of tritium fluctuations in fractured basalts, *Water Resour. Res., 23*(5), 894–902, 1987.

Eagleson, P. S., R. Mejia-r, and F. March, Computation of optimum realizable unit hydrographs, *Water Resour. Res., 2*(4), 755–764, 1966.

Goltz, M. N., Three-dimensional analytical modeling of diffusion-limited solute transport, Ph.D. dissertation, Stanford Univ., Stanford, Calif., 1986.

Himmelblau, D. M., and K. B. Bischoff, *Process Analysis and Simulation: Deterministic Systems*, John Wiley, New York, 1968.

Jury, W. A., G. Sposito, and R. E. White, A transfer function model of solute transport through soil, 1, Fundamental concepts, *Water Resour. Res., 22*(2), 243–247, 1986.

Kanasewich, E. R., *Time Sequence Analysis in Geophysics*, 2nd ed., Univ. of Alberta Press, Edmonton, 1975.

Knisel, W. G., Response of karst aquifers to recharge, *Hydrol. Pap. 60*, Colo. State Univ., Ft. Collins, 1972.

Laurenson, E. M., and T. O'Donnell, Data error effects in unit hydrograph derivation, *J. Hydraul. Div. Am. Soc. Civ. Eng., 95*(HY6), 1899–1917, 1969.

Neuman, S. P., and G. de Marsily, Identification of linear systems response by parametric programming, *Water Resour. Res., 12*(2), 253–262, 1976.

Passioura, J. B., Hydrodynamic dispersion in aggregated media, 1, Theory, *Soil Sci., 111*, 339–344, 1971.

Priestley, M. B., *Spectral Analysis and Time Series*, Academic, San Diego, Calif., 1981.

Rao, P. S. C., E. E. Rolston, R. E. Jessup, and D. M. Davidson, Solute transport in aggregated porous media: Theoretical and experimental evaluation, *Soil Sci. Soc. Am. J., 44*, 1139–1146, 1980.

Rinaldo, A., and G. Gambolati, Basin-scale transport of dissolved species in groundwater, paper presented at Adv. Res. Workshop, NATO, Lisbon, Portugal, June 2–6, 1987.

Shuster, E. T., and W. B. White, Seasonal fluctuations in the chemistry of limestone springs: A possible means for characterizing carbonate aquifers, *J. Hydrol., 14*, 93–128, 1971.

Thornthwaite, C. W., and J. R. Mather, Instructions and tables for computing potential evapotranspiration and the water balance, *Pub. Climatol., Drexel Inst. Technol., 10*(3), 1957.

Valocchi, A. L., Validity of the local equilibrium assumption for modeling sorbing solute transport through homogeneous soils, *Water Resour. Res., 21*(6), 808–820, 1985.

Vandike, J. E., The effects of the November 1981 liquid-fertilizer pipeline break on groundwater in Phelps County, Missouri, Open File Report, Mo. Dep. Nat. Resour., Rolla, 1982.

S. J. Dreiss, Department of Earth Sciences, Applied Sciences Building, University of California, Santa Cruz, CA 95064.

(Received June 28, 1988;
accepted July 7, 1988.)